

Simulation of Elliptical Vibration Cutting Process with Thin Shear Plane Model

Eiji Shamoto¹, Norikazu Suzuki¹ and Rei Hino¹
¹Department of Mechanical Science and Engineering
 Nagoya University
 Nagoya, Aichi, Japan

INTRODUCTION

The elliptical vibration cutting was first proposed in 1993 [4-7]. Since then, some ultrasonic elliptical vibration tools have been developed, and their machining performance has been investigated for some difficult-to-cut materials [8, 9, 13]. Recently, this technology has been tested in industries mainly for ultraprecision diamond cutting of dies, molds, and optical parts.

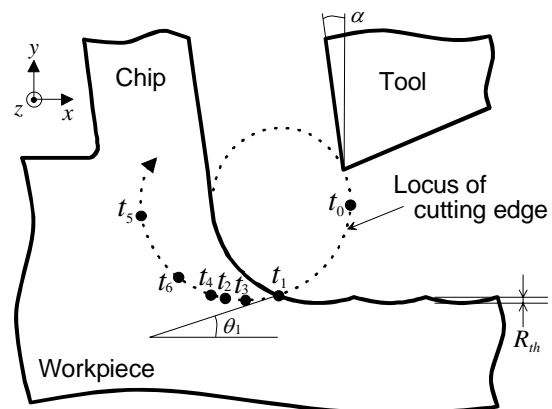
On the other hand, there have been less investigations on basic mechanics of the elliptical vibration cutting. An analytical model of the orthogonal elliptical vibration cutting process, in which all velocities, forces and vibrations are perpendicular to the cutting edge, was developed and verified experimentally to predict theoretical roughness, critical relief angle, shear angle, etc., and to clarify effects of speed ratio, i.e. maximum vibration speed in the nominal cutting direction / the nominal cutting speed, vertical vibration amplitude and phase difference between the two directional vibrations [7]. However, the practically applied processes are not generally the orthogonal type. The elliptical vibration locus is usually inclined around the cutting direction in most of the industrial applications.

Therefore, simple analytical models of the three dimensional (3D) elliptical vibration cutting processes are proposed in the present research in order to simulate the process quickly and to understand the basic mechanics. The results simulated with the present models are compared with experimental data published in the previous papers [7, 12].

ELLIPTICAL VIBRATION CUTTING PROCESS WITH UNIQUE PHENOMENON OF FRICTION

Figure 1 shows a schematic illustration of the elliptical vibration cutting process. The cutting starts at the time t_1 , and the small part left in the previous cycle is cut at small depth until the time t_2 , when the rake face contacts with the chip formed in the previous cycle. In the actual process, this small part may be burnished and pushed into the workpiece and the chip because

of cutting edge roundness. After the time t_2 , the workpiece material is sheared and removed as the chip at large depth of cut. As the tangent of cutting path exceeds the shear direction at the time t_6 , the frictional direction is reversed. In the actual process, the tool moves together with the chip in the shear direction near t_6 without the sudden reversal of friction because of elasticity. Then, the tool is separated from the chip at the time t_5 , when the tangent is parallel to the rake face. The reduced or reversed friction leads to significant reduction of cutting force, energy and heat generation [4-6].



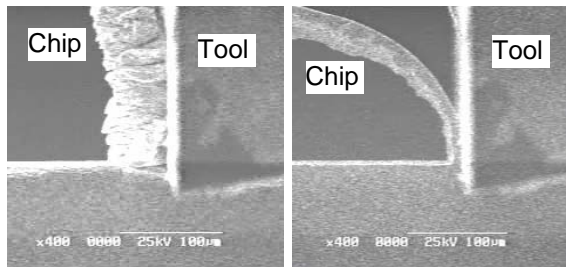
- | | |
|--|------------------------------------|
| t_0 : $t=0$ | t_6 : Reversal of friction |
| t_1 : Beginning of cutting | t_5 : End of cutting |
| t_2 : Contact between rake face and chip | θ_1 : Critical relief angle |
| t_3 : Bottom of locus | R_{th} : Theoretical roughness |
| t_4 : End of finished surface generation | |

FIGURE 1. Elliptical vibration cutting process.

Figure 2 shows the chip formation processes of orthogonal ordinary cutting and elliptical vibration cutting. It shows that the chip thickness is much smaller in the elliptical vibration cutting though the cutting conditions are the same. Figure 3 shows the cutting forces measured in the both processes. The negative thrust force shown in Fig. 3(b) indicates the reversal of friction, and this leads to the significant increase of shear angle, see Fig. 2, and the significant

reduction of cutting force, see Fig. 3 [4-6].

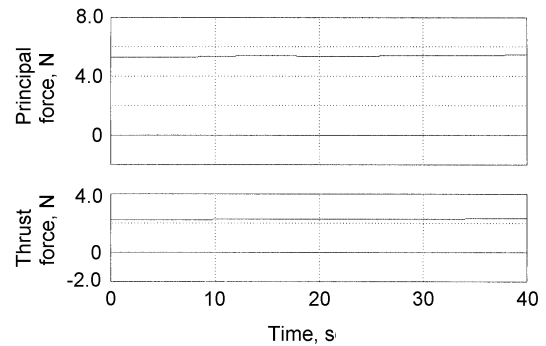
Figure 4 shows typical chips observed in practical ultraprecision elliptical vibration cutting with single crystal diamond tools. The chips are usually continuous and the chip thickness is almost constant as shown in the figures, although the instantaneous cutting direction is varied. This suggests that the shear deformation may be caused by average or total force applied to the workpiece material in one cycle of the elliptical vibration.



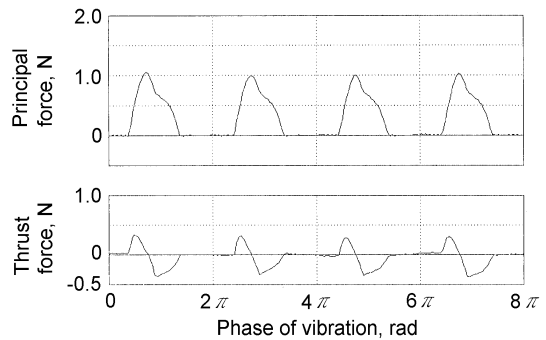
(a) Ordinary cutting (b) Elliptical vib. cutting
 [Conditions] Workpiece: Copper, rake: 0 deg, cutting speed: 0.26 mm/min, depth of cut: 10 μm , elliptical vibration: circular, amp.: 10 μm_{p-p} , freq.: 1.2 Hz
 FIGURE 2. Direct observation of chip formation processes.

As mentioned above, the elliptical cutting process can be divided into the two processes, i.e. the micro cutting or burnishing process from t_1 to t_2 and the cutting process with the reduced or reversed friction from t_2 to t_5 . When the depth of cut is large enough relatively to the vertical amplitude of vibration, the former micro machining period is negligible. On the other hand, when the depth is extremely small and the cutting edge is sharp enough, the latter cutting period vanishes, and the process may be similar to micro milling except that the rake face is not inclined during cutting and that the tool path is elliptical.

Judging from the observations of process and chips, it is considered that the constant continuous chip formation with the unique frictional phenomenon is the main process in many of the practical elliptical vibration cutting. Whereas the mechanism of the former micro machining can be understood as the ordinary micro machining process, the latter chip formation process with the reversed or reduced friction is unique and academically interesting. Therefore, the former process is not considered and the latter process is modeled and discussed in the present research.



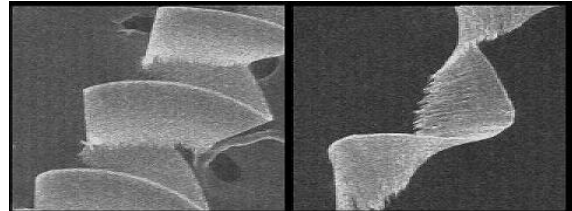
(a) Ordinary cutting



(b) Elliptical vibration cutting

[Conditions] Same as Fig. 2

FIGURE 3. Transient cutting forces measured in ordinary cutting and elliptical vibration cutting.



[Conditions] Workpiece: hardened steel, tool: R1 mm, rake: 0 deg, cutting speed: 2.5 m/min, depth of cut: 10 μm , feed rate: 10 $\mu\text{m}/\text{rev}$, vibration: circular, amp.: 10 μm_{p-p} , freq.: 20 kHz
 FIGURE 4. Chips formed by ultraprecision elliptical vibration cutting.

For simplicity, the cutting edge is assumed sharp enough, and the elastic deformation is neglected. The instantaneous depth of cut is decreased gradually during the latter cutting period, but this effect is also neglected, i.e. the depth is assumed constant. The simple thin shear plane model is employed, and the maximum shear stress and minimum energy principles are separately applied for simple simulations and better comprehension of the continuous chip formation process. The above issues neglected here may be considered in the

future for more precise analysis and comprehension.

GEOMETRY OF 3D ELLIPTICAL VIBRATION CUTTING PROCESS

Figure 5 shows various types of elliptical vibration cutting. Figure 5(a) is the orthogonal type. Figure 5(b) is the oblique type which is intermittent cutting with sidewise motion of the cutting edge or a rotary tool on average, which is equivalent to oblique cutting with reduced width of cut [10-12]. In this case, the friction is not reduced, but the cutting force is reduced by the reduction of actual width of cut [11]. This is why knives are pulled in the cutting edge direction to reduce the force.

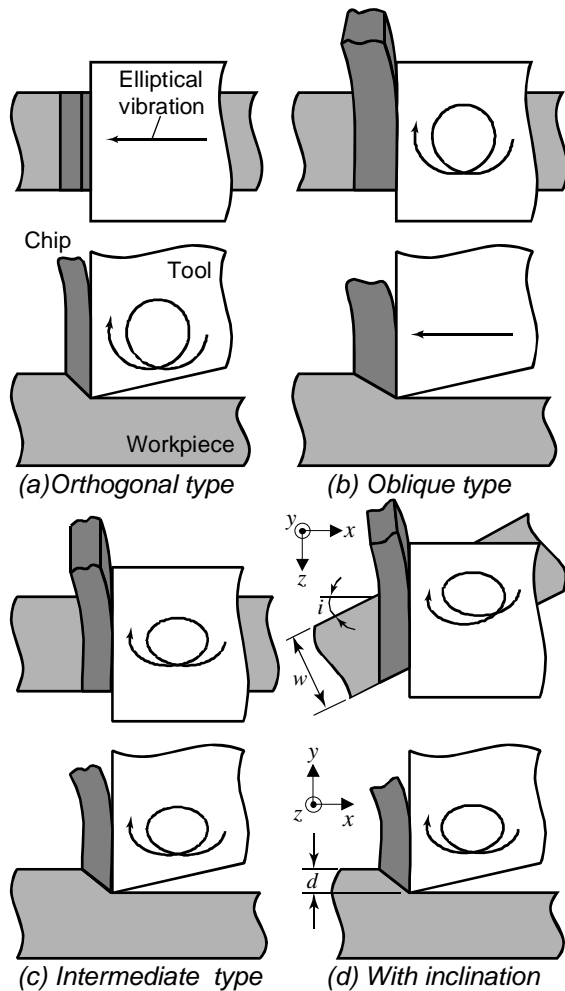


FIGURE 5. Various types of elliptical vibration cutting processes.

Figure 5(c) shows intermediate type between the above two types, which has both effects, i.e. the thrust force is reduced or reversed and the

actual width of cut is reduced. This intermediate type is utilized widely in practice. Furthermore, the cutting edge is not always perpendicular to the cutting direction, as shown in Fig. 5(d), where the obliquity of cutting direction is denoted by an inclination angle i . In this case, the inclination of cutting direction enhances obliquity of the inclined elliptical vibration.

The tool is vibrated at an angular frequency ω and fed at a nominal cutting speed V_c , and the workpiece is stationary here. Then, the tool path with the vibration can be expressed as follows.

$$\begin{aligned} x(t) &= a \cos(\omega t) - V_c t \cos i \\ y(t) &= b \cos(\omega t + \varphi_y) \\ z(t) &= c \cos(\omega t + \varphi_z) + V_c t \sin i \end{aligned} \quad (1)$$

where x , y and z are Cartesian coordinates of the relative position between the tool and the workpiece in the direction normal to the cutting edge, the thrust direction and the cutting direction respectively, see Fig. 1 and Fig. 5(d). The nominal cutting direction lies on the x - z plane, i.e. finished surface. a , b and c are vibration amplitudes in the x , y and z directions respectively. t is time and φ_y and φ_z are phase shifts of the vibrations in the y and z directions respectively.

When the minimum relative speed in the direction normal to the rake face is negative, the cutting process becomes intermittent.

$$\begin{aligned} &V_c \cos i \cos \alpha \\ &- \omega \sqrt{(a \cos \alpha - b \sin \alpha \cos \varphi_y)^2 + (b \sin \alpha \sin \varphi_y)^2} < 0 \end{aligned} \quad (2)$$

where α is the normal rake angle which is the rake angle in the plane normal to the cutting edge.

Under this intermittent condition, the time t_5 (see Fig. 1) is obtained by solving Eq. (3), since the relative speed in the direction normal to the rake face becomes zero at t_5 .

$$\begin{aligned} &\{a\omega \sin(\omega t_5) + V_c \cos i\} \cos \alpha \\ &- b\omega \sin(\omega t_5 + \varphi_{xy}) \sin \alpha = 0 \end{aligned} \quad (3)$$

The rake face is separated from the chip at t_5 , and then it comes back to the same plane at t_2+T , where T is a vibration period. Thus, t_2 can be solved numerically by the following equation.

$$\begin{aligned}
& \{x(t_2 + T) - x(t_5)\} \cos \alpha + \{y(t_5) - y(t_2 + T)\} \sin \alpha = 0 \\
\therefore & a \{ \cos(\omega t_2) - \cos(\omega t_5) \} \cos \alpha \\
& + b \{ \cos(\omega t_5 + \varphi_y) - \cos(\omega t_2 + \varphi_y) \} \sin \alpha \quad (4) \\
& = V_c (T - t_5 + t_2) \cos \alpha \cos i
\end{aligned}$$

The other parameters t_1 , t_3 , t_4 , θ_1 and R_{th} can also be solved in a similar way to the orthogonal elliptical vibration cutting [4].

PREDICTION OF SHEAR DIRECTION IN 3D ELLIPTICAL VIBRATION CUTTING PROCESS

The shear direction in the 3D vibration cutting process is assumed to be constant, judging from the direct observation of the process and the chips obtained in the practical cutting operations as mentioned above. The shear direction is predicted by extending the 3D thin shear plane model [10,11] as follows.

As the shear direction \vec{v}_s (unit vector) is constant, the chip also moves in the same direction independently of the instantaneous tool velocity \vec{V}_T , i.e. instantaneous cutting velocity. Thus, the instantaneous velocity of the chip material \vec{V}_M is derived by:

$$\vec{V}_M = |\vec{V}_M| \vec{v}_s = \frac{\vec{V}_T \cdot \vec{n}}{\vec{v}_s \cdot \vec{n}} \vec{v}_s \quad (5)$$

where \vec{n} is a unit vector normal to the rake face and given by $(-\cos \alpha, \sin \alpha, 0)$, and \vec{V}_T is given by the time-derivative of tool position:

$$\vec{V}_T = (-a\omega \sin(\omega t) - V_c \cos i, -b\omega \sin(\omega t + \varphi_y), -c\omega \sin(\omega t + \varphi_z) + V_c \sin i) \quad (6)$$

The friction \vec{f} (unit vector) acts in the opposite direction of the relative motion between the tool and the chip.

$$\vec{f} = \frac{\vec{V}_T - \vec{V}_M}{|\vec{V}_T - \vec{V}_M|} \quad (7)$$

Then, the direction of resultant cutting force \vec{r} (unit vector) can be obtained as follows, assuming a constant frictional angle β .

$$\vec{r} = \vec{n} \cos \beta + \vec{f} \sin \beta \quad (8)$$

The resultant force \vec{R} needs to produce the shear force F_s in the shear plane, and hence it can be calculated by:

$$\vec{R} = \frac{F_s}{\vec{r} \cdot \vec{v}_s} \vec{r} = \frac{\tau w d \sqrt{(\vec{v}_s \cdot \vec{e}_y)^2 + (\vec{v}_s \cdot \vec{e}_x)^2}}{(\vec{v}_s \cdot \vec{e}_y)(\vec{r} \cdot \vec{v}_s) \cos i} \vec{r} \quad (9)$$

where τ is shear stress in the shear plane, w and d are the width and depth of cut, see Fig. 5(d), and \vec{e}_x and \vec{e}_y are unit vectors in the x and y directions respectively. This force is varied with the varying cutting velocity \vec{V}_T , and thus the instantaneous cutting power U is given by:

$$U = \vec{R} \cdot \vec{V}_T \quad (10)$$

The shear direction is predicted with the two fundamental principles separately. One is the maximum shear stress principle. It is assumed that the shear occurs in the maximum shear stress direction, where the resultant force makes 45 degrees with the shear direction and also the shear plane [10,11]. In the present 3D vibration cutting process, the resultant force is varied. Therefore, it is assumed that the shear direction is determined by summation of the instantaneous resultant force \vec{R}_{sum} during the cutting period from t_2 to t_5 .

$$\vec{R}_{sum} = \sum |\vec{V}_M| \vec{R} \quad (11)$$

where $|\vec{V}_M|$ is multiplied in the present paper as a weight function, because the influence on the shear deformation may be increased as the removed material is increased. As a result, the shear direction \vec{v}_s and the summed force \vec{R}_{sum} need to satisfy the following equation.

$$\frac{\vec{R}_{sum}}{|\vec{R}_{sum}|} = \vec{v}_s \cos 45^\circ + \vec{n}_s \sin 45^\circ \quad (12)$$

where \vec{n}_s is a unit vector normal to the shear plane and given by:

$$\vec{n}_s = \frac{\vec{v}_s \times \vec{e}_y}{|\vec{v}_s \times \vec{e}_y|} \quad (13)$$

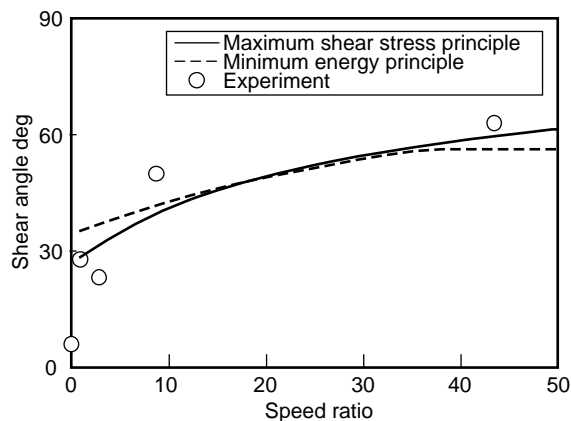
Therefore, the correct shear direction \vec{v}_s can be searched as follows. First, \vec{R}_{sum} is calculated by Eqs. (5-11), and then \vec{v}_s is checked by Eqs. (12, 13). If the error between the left and right sides of Eq. (12) is not small enough, the shear direction \vec{v}_s is updated. The correct vector is searched numerically by the iteration.

The other fundamental shear angle prediction is based on the minimum energy principle. The shear direction is determined here so that the total cutting energy E becomes minimum, where E is given by integrating instantaneous cutting power numerically from t_2 to t_5 as follows.

$$E = \sum U \Delta t \quad (14)$$

Thus, solution of the shear direction \vec{v}_s can be found by searching \vec{v}_s iteratively so that the energy becomes the minimum.

The above analytical models are applied to simulation of the 3D elliptical vibration cutting process here. However, the models are also valid for other cutting processes including the 3D linear vibration cutting where constant continuous chips are formed. The present models give the same solutions as the oblique cutting models [10,11] when $i \neq 0$ and $a=b=c=0$, and they yield to Merchant's [2] and Krystof's [1] (or Lee-Shaffer's [3]) models when i is also zero.



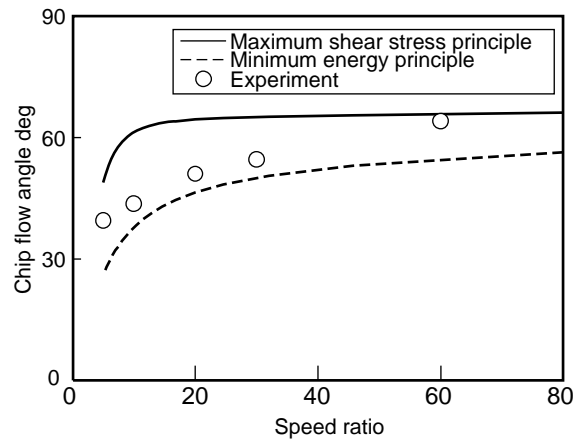
[Conditions] Same as Fig. 2

FIGURE 6. Shear angles at various speed ratios in orthogonal type of elliptical vibration cutting.

SIMULATION RESULTS AND DISCUSSIONS

The developed analytical models are applied to the orthogonal and oblique types of elliptical vibration cutting, and simulated results are compared here with some published data.

Figure 6 shows the shear angles predicted and measured [7] at various speed ratios in the orthogonal type. The friction angle β utilized in the simulation is identified 23.5 deg by the forces measured in the ordinary cutting, see Fig. 3(a). Figure 7 shows the chip flow angles predicted and measured [12] at various speed ratios in the oblique type of elliptical vibration cutting. β is 41.3 deg [12] in the simulation.



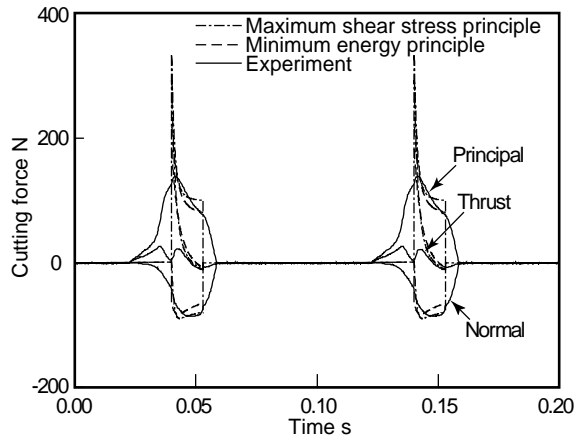
[Conditions] Workpiece: aluminum, rake: 0 deg, depth of cut: 50 μm , vibration: circular, amp.: 1 mm_{p-p}, freq.:10 Hz

FIGURE 7. Chip flow angles at various speed ratios in oblique type of elliptical vibration cutting.

Considering the simplicity of analytical models, the characteristic angles predicted with either principle agree roughly with the experimental data, as shown in the figures. It shows that the two types of elliptical vibration cutting process can be predicted quickly and roughly with the models developed here. The rough agreements suggest that the orthogonal and oblique types of elliptical vibration cutting can be understood as the unique chip formation process with reversal of friction and the oblique cutting with the reduced width of cut respectively.

Transient cutting forces in the intermediate type are also predicted and compared with experimental data [12] in Fig. 8. β is 41.3 deg and τ is 94.3 MPa [12]. The results are in a good agreement during the cutting period, as shown in the figure. The disagreement is considered to be caused mainly by the elastic deformation, which is neglected here. The thrust force is reversed in the cutting period by the orthogonal component of the elliptical vibration. The force in the cutting edge direction, which is shown by "normal" in the figure, corresponds to the

obliquity of cutting process. This is caused by the oblique component of the elliptical vibration, and it also reduces the cutting force by reducing the actual width of cut [11]. The measured peak principal force was 140 N as shown in the figure, while average principal force measured in the ordinary cutting was 480 N [12]. It is considered that this significant reduction is caused by combination of the above two effects.



[Conditions] Workpiece: aluminum, rake: 0 deg, depth of cut: 0.3 mm, width of cut: 2mm, cutting speed: 94.3 mm/min, vibration: circular, amp.: 1 mm_{p-p}, freq.:10 Hz, inclination of elliptical vibration: 80 deg from orthogonal type, i.e. 10 deg from finished surface

FIGURE 8. Transient cutting forces in intermediate type of elliptical vibration cutting.

CONCLUSION

The simple analytical models of the 3D elliptical vibration cutting are developed by employing the thin shear plane model and either the maximum shear stress principle or the minimum energy principle. The simulated results agree roughly with the experimental data published previously. The models represent the unique cutting mechanics of two types of elliptical vibration cutting. The simplified models and the simulated and experimental data are helpful to understand the processes. They suggest that the continuous chip formation process in the oblique type of elliptical vibration cutting is the unique cutting process with the reversal phenomenon of friction, and the oblique type of elliptical vibration cutting is equivalent on average to the cutting process with the sidewise motion of tool. The practical elliptical vibration cutting can be understood as the intermediate process between the two types.

REFERENCES

- [1] Krystof J. Berichte uber Betriebswissenschaftliche Arbeiten, Bd., 12, VDI Verlag: 1939
- [2] Merchant M.E. Mechanics of the Metal Cutting Process. II. Plasticity Conditions in Orthogonal Cutting. J. Applied Physics: 1945; 16: 318-324
- [3] Lee, E.H., Shaffer B.W. The Theory of Plasticity Applied to a Problem of Machining. J. Applied Mechanics: 1951; 18; 405-413
- [4] Shamoto E., Moriwaki T. Fundamental Study on Elliptical Vibration Cutting. Proc. 8th Annual Meeting, ASPE: 1993; 162-165
- [5] Shamoto E., Moriwaki T. Study on Elliptical Vibration Cutting. Ann. CIRP: 1994; 43/1: 35-38
- [6] Shamoto E., Morimoto Y., Moriwaki T. Elliptical Vibration Cutting (1st Report, Cutting Principle and Basic Performance) (in Japanese). J. JSPE: 1996; 62/8: 1127-1131
- [7] Shamoto E., Morimoto Y., Moriwaki T. Elliptical Vibration Cutting (2nd report, Study on Effects of Vibration Conditions) (in Japanese). J. JSPE: 1999; 65/3: 411-417
- [8] Shamoto E., Moriwaki T. Ultraprecision Diamond Cutting of Hardened Steel by Applying Elliptical Vibration Cutting. Ann. CIRP: 1999; 48/1: 441-444
- [9] Shamoto E., Ma C.X., Moriwaki T. Ultraprecision Ductile Cutting of Glass by Applying Ultrasonic Elliptical Vibration Cutting. Proc. of 1st Int. Conf. and general meeting of EUSPEN: 1999; 408-411
- [10] Shamoto E., Altintas Y. Prediction of Shear Angle in Oblique Cutting with Maximum Shear Stress and Minimum Energy Principles. Trans. ASME J. Manuf. Sci. Eng.: 1999; 121: 399-407
- [11] Shamoto E. Study on Three Dimensional Cutting Mechanics (1st Report, Comprehension and Vector Formulation of Oblique Cutting Process) (in Japanese). J. JSPE: 2002; 68/3: 408-414
- [12] Shamoto E., Song Y.C., Sassa K., Yoshida H., Hino R., Moriwaki T. Proposal of Oblique Type of Elliptical Vibration Cutting and Its Basic Performance. J. JSPE: 2003; 69/7: 970-975
- [13] Suzuki N, Haritani M, Yang J., Hino R., Shamoto E. Elliptical Vibration Cutting of Tungsten Alloy Molds for Optical Glass Parts. Ann. CIRP: 2007; 56/1: to be published